20th Australasian Fluid Mechanics Conference
Perth, Australia
5-8 December 2016

Flow structures generated by elongated plates settling in a water column

H. Sørensen*, A.L. Jensen and J. Hærvig

Department of Energy Technology,
Aalborg University, Aalborg DK-9220, Denmark

Abstract

In order to establish a mathematical formulation of the equation of motion, the trajectory of particles settling in a stagnant fluid has been studied for generations. The publication by Field et al. [4] is one of the more well-known studies, where the dynamic behaviour of disks as function of the dimensionless moment of inertia and Reynolds number was investigated. The objective of the present work is to collect and present experimental data about the flow structures generated by the settling of elongated plates in a water column. The experiments are carried out by releasing the plates at an initial angle of 15° in a 0.60 m x 0.30 m × 0.35 m (L×B×H) glass container filled with water. Continuous Particle Image Velocimetry is used to analyse both the velocity field of the continuous phase and the motion of the plates. The experiments show a well-defined oscillating motion of the plate. A stall occurs each time the plate changes horizontal direction of motion. The results show a flow building up when the plate accelerates and a vortex rolling off in each turn.

Introduction

For generations the motion of flat bodies rising or falling in a viscous media has been target for numerous researchers. Maxwell (1853) did a pioneering effort in considering the fluid structure interaction [9]. The thoughts provided by Maxwell enabled us to understand the mechanism behind the motion without leading to a general solution to the problem [5]. In the later twentieth century objects with different forms and sizes were utilised in newer research on the same topic. The experiments were typically filmed and analysed afterwards [2,11]. With the invention of the digital video camera, this became an easy task and a lot of research was published with detailed information about the trajectory itself [1,7,12]. Simultaneously with the experimental research on the field, numerous researchers have put effort in calculating the trajectories either by simple numerical models or computational fluid dynamics [3,7]. Andersen et al. (2005) had probably the best known solution to unsteady aerodynamics of freely falling plates in a quasi-two-dimensional flow. They utilised two-dimensional direct numerical simulations to calculate the flow field around the plate and the motion of the plate itself. One of the conclusions from Andersen et al. (2005) is that the fluid forces that build up on a freely falling plate depend sensitively on the precise location of vortices and low-pressure regions. With this in mind, it is crucial to extend the experimental investigations to include simultaneous measurements of both object trajectories as well as fluid motion. Recently, a few researchers have addressed focus to this in their papers. Vetchanin and Klenov (2015) concluded that there was a disagreement between measured and computed oscillations by Andersen et al. [10]. Huang et al. (2013) concluded in their paper that more data is needed for further analysis of the relationship between forces on the objects and the fluid motion [6].

The main scope of this present work was to investigate the flow structures generated by freely falling plates. For this purpose continuous Particle Image Velocimetry (PIV) is used.

Trajectories of Objects Settling in a Fluid

A body released in a fluid either raises or settles depending on the density ratio between the body and the fluid. For both cases, the closer the density ratio is to one, the more important the unsteady fluid forces introduced by the relative motion between the fluid and the object itself become. In the case of a large density ratio the object accelerates to a certain velocity, where the drag and lift forces become dominant – and a moment will be generated if the aerodynamic centre is located away from the centre of gravity. Depending of the Reynolds number and dimensionless (mass) moment of inertia, the object may obtain a tumbling motion or go into a chaotic/periodic motion. For falling disks, Field et al. (1997) mapped different regimes in a plot [4]. In this study the disks are replaced by flat elongated plates which are assumed to settle with similar regimes. With that in mind the plates are expected to settle in a steady regime at low Re. At higher Re, the motion depends on the dimensionless moment of inertia.

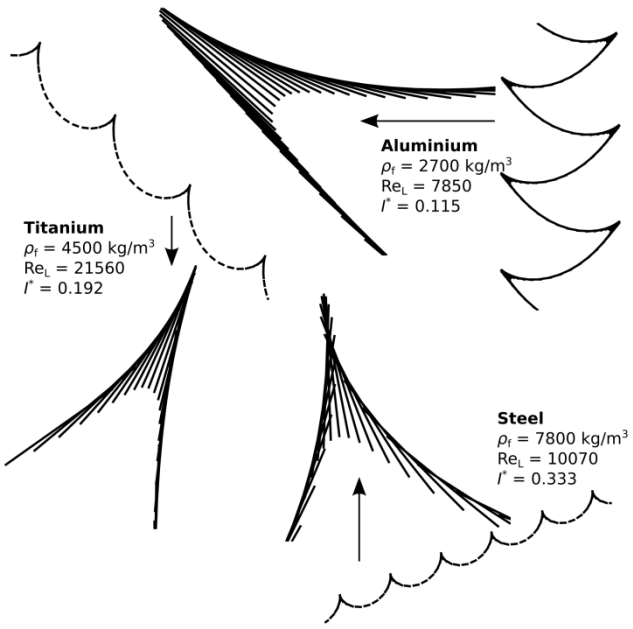

Figure 1: Examples of plates trajectories for different dimensionless moment of inertia Reprinted with permission [8].

* Corresponding author. E-mail address hs@et.aau.dk

A common mapping with dimensionless moment of inertia (I^*), and Reynolds number (Re), as main features are adapted by the majority of researchers in the field. For a 2 dimensional case where the plate width (W) is much larger than the length (L). The dimensionless moment of inertia is a function of plate thickness (H), length of the plate (L), fluid density (ρ_f) and plate material density (ρ_p).

$$I^* = \frac{8 \cdot \rho_p \cdot H \cdot (L^2 + H^2)}{3 \cdot \pi \cdot \rho_f \cdot L^3} \quad (1)$$

The Reynolds number of the plate is given as the ratio of inertial forces to viscous forces in the fluid.

$$Re = \frac{u \cdot L \cdot \rho_f}{\mu_f} \quad (2)$$

Where u is the mean vertical disk velocity and μ_f is the dynamics viscosity of the fluid. Also the 2D-aspect ratio (β) is an important identifier of plates raising or settling in a quiescent fluid.

$$\beta = \frac{H}{L} \quad (3)$$

Experimental Apparatus and Methods

The experiments are carried out by releasing a plate from an initial angle of 15° in a rectangular water tank (figure 3). A release mechanism is mounted on the top of the water tank which holds plate in the same position and angle in all experiments. The release mechanism is constructed in a way, so there is a minimum area in contact with the plate. This allows the plate to be submerged in water and reduces the influence of the initial conditions at release. In the experiment the plates are released so they only rotate about their major axis z' and settle with a two-dimensional trajectory.

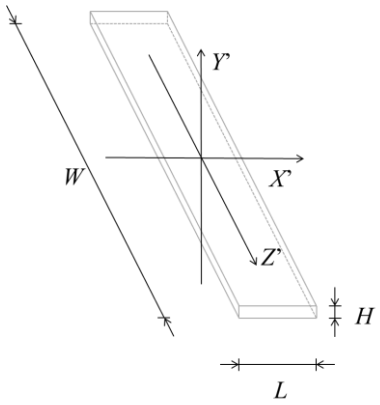

Figure 2: Particle coordinate system. The Z' axis is defined as the particle major axis. The particle is expected to rotate about this axis. The particle translation is in the plane defined by the X' and Y' axis.

The flow field is seeded by Rhodamine B coated polyamide particles with a diameter of 1-20µm and illuminated by a green continuous laser (CNI Laser MGL-W-532, 5W). The illuminated flow and plates are filmed by a camera mounted with a red-bandpass filter. The camera is positioned in different positions (2m to 4m from measurement plane) in order to adjust the Field Of View (FOV) to the generated flow structures and plate trajectory. A Basler Aca1920-155um cmos camera mounted with a Sigma DGMACRO 105mm, F/2.8 lens is used to capture the entire flow field and the plate as well.

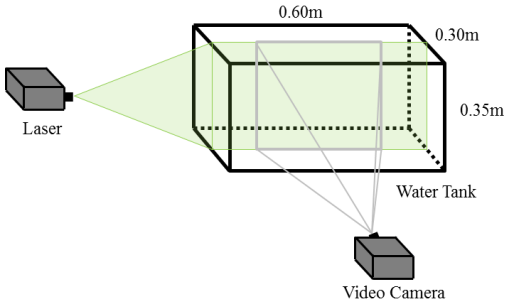

Figure 3: Sketch of the experimental setup used in the experiments.

The recorded images contain information about both the seeded flow field and the plate. The plate motion is analysed by an in-house software made in LabVIEW Vision, where the plate position and angle is determined and saved for each time step in the data series. The processing steps in the software are presented in figure 3.

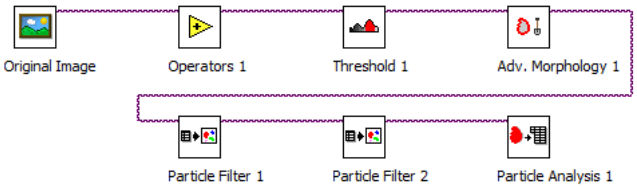

Figure 4: Processing steps in software for extraction of plate position and angle in individual images.

The raw images of the seeded fluid flow field is analysed in DynamicStudio 2015a from Dantec Dynamics. The Adaptive Correlation method is used with initial IA size 64×64 pixels and two refinement steps ending up with a final IA size of 16×16 pixels. The processing is done with subpixel accuracy and deforming windows. The validation criterion is minimum peak height relative to a peak height of 1.25. A moving area filter of 3×3 with an acceptance criteria of 0.15 is used for local neighbourhood validation, and the central difference method is used for interrogation area offset. In the experiments three different aluminium plates are used with the following specifications.

H [mm]	L [mm]	$1/\beta$ [-]	I^* [-]	ρ [kg/m^3]
2.10	40.1	19.1	0.120	2700
2.10	35.0	16.7	0.138	2700
2.10	30.4	14.5	0.159	2700

Table 1: Plate thickness H, plate length L, 2D-aspectratio β, dimensionless moment of inertia I^* and material density ρ.

Results

An oscillating trajectory is seen for all three plates. For the 2mm x 40mm plate the trajectory corresponds very well to the presented trajectory of an aluminium plate in figure 1 (top right). During the experiments it is noticed that when the dimensionless moment of inertia is increased the particle starts drifting to the side while the zig-zag motion is maintained. The plate has a clockwise rotation in turns where the plate is moving from right to left and stalls followed up by a motion from left to the right (figure 5 positions A and C). The plate rotation is counter clockwise when the plate enters a turn from left to right and back (figure 5 position B).

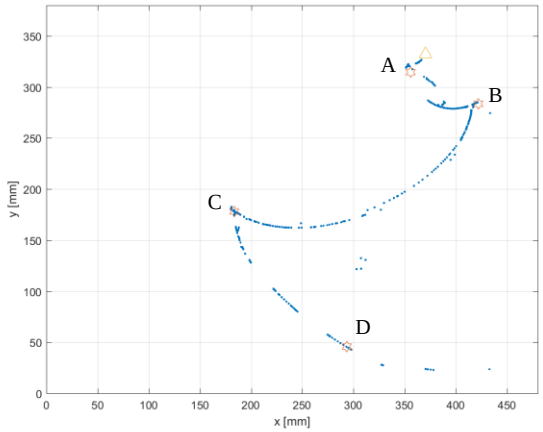

Figure 5: Trajectory formed by plotting the centre position to running time of the 2mm x 40mm plate. Blue dots: Plate path line. Yellow triangle: Start position of the plate. Orange stars: Plate centre position to given time after release (A: 200ms, B: 530ms, C: 1088ms & D: 1402ms after release) - flow structures are given in figure 6-9 for the four positions.

The analysis of the plate position and angle show that the maximum rotational velocity of the plate occurs roughly a tenth of a second before the turning point. The exact time varies with plate dimension, see table 2.

H [mm]	L [mm]	θ_{Turn}[deg]	ϖ_{max}[rad/s]	Δt [ms]
2.10	40.1	-55	-4.5	117
2.10	35.0	-60	-5.5	103
2.10	30.4	-65	-6.5	90

Table 2: Plate thickness H, plate length L, turning angle θ_{Turn}, angular velocity ϖ_{max}, time between max angular velocity and turn angle Δt.

Flow Structures Created by a Plate Settling in Water

For the 2mm x 40mm plate the first turn, 'A' in figure 5, occurs 200ms after release. The PIV measurements in figure 6 reveal a formation of two vortices with clockwise and counter clockwise rotation. The two vortices are created at the ends of the plates when the plate starts to settle almost vertical down from the release mechanism.

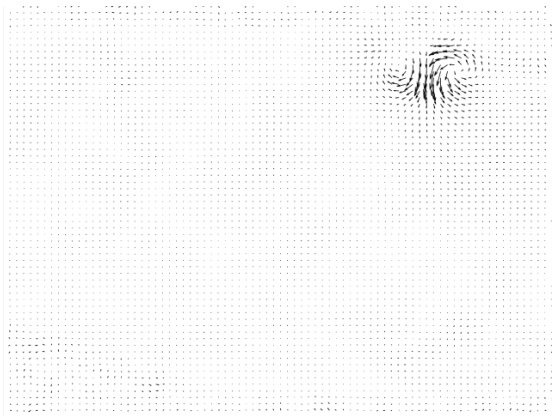

Figure 6: Vortices created when the plate is released.

From position 'A' the plates moves to the right and experiences the second stall 530ms after the release at position 'B' in figure 5. A new vortex rotating counter clockwise is created. The first vortex created in turn 'A' is still present in the measurements.

Figure 7: Vortex created 530ms after plate release.

At 1088ms after release the plate enters the third turn at position 'C' and a new clockwise rotating vortex is formed. The two earlier formed vortices are still present in top right corner of figure 8.

Figure 8: Vortex created 1088 ms after plate release.

Figure 9 show the flow field 1402ms after the release of the plate. The three created vortices are still visible and it is also possible to see flow vectors created along the particle path line. For the other two plate dimensions similar motion pattern are observed but with other locations of turning points. For both plates a vortex is formed in each turning point.

Figure 9: Vortex created 1402ms after plate release.

Tangential Velocities of Vortices Created at 3rd Turn

For the three plate dimensions investigated in this paper figures 11, 12 and 13 show the tangential velocity along a horizontal line through centre of the vortex created at turning point 'C' (see figure 5 for location).

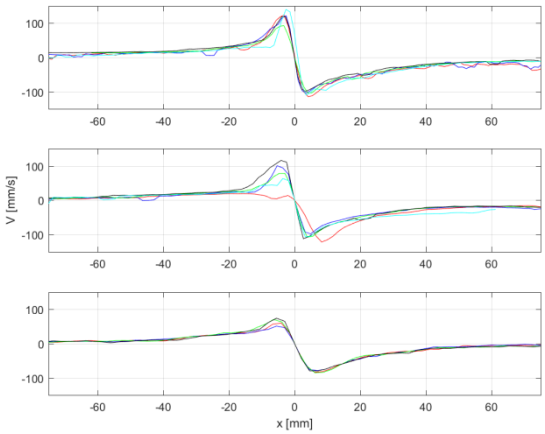

Figure 10: Tangential velocity of created vortex at turning point C for the three aluminium plates used in this experiment. Top: plate dimension 2mm x 40mm. Middle: plate dimension 2mm x 35mm. Bottom: plate dimension 2mm x 30mm.

Discussion

The plate moves from one turning point towards the next turning point while a viscous flow is building up relative to the plate. The flow is almost symmetric on the upper and lower sides of the plate during the period, where the plate accelerates from a turn to the position, where the plate reaches a horizontal orientation. After this position the incident angle continues to increase and the flow starts to move around the leading edge from downward to the upper side of the plate. This motion of the fluid combined with the rotation of the plate results in a vortex building up every time the plate enters a turn and shifts its direction of motion. The current results show that the maximum tangential velocity of the vortex is largest for the plate with the biggest aspect ratio. The results based on image analysis show on the other hand lowest rotational velocity for the plate with largest aspect ratio. This indicates that the plate dimension has larger effect on the strength and size of the created vortex than the rotational speed of the plate in the turning point. At the turning point (point 'C' in figure 5) the plate stops its translation and rotates about a point located very close to the leading edge of the plate (defined by direction of motion in to the turn). The turning point of the plate is also the centre of the created vortex. It should also be noticed that the vortices created only moves very slowly in the direction of the created particle wake.

Conclusions

In this paper an experimental study of the unsteady flow around a freely settling aluminium plate is presented. Three different plate dimensions have been used in the experiments, and all three trajectories belong to the category of periodic motion. The measurements show a clearly defined vortex at every turning point in the trajectory. With the contribution of the results from this research, quantitative data for the local flow field around the plate is now available. Next step is to narrow down the window of the measurement area to be able to obtain accurate information about the boundary layer along the plate for different positions in the trajectory. A variation of plate dimensions and dimensionless moments of inertia might also be of interest for those who are looking for experimental data to verify their numerical models.

Acknowledgments

Otto Mønsteds Foundation is supporting this work by a travel grant.

References

[1] Andersen, A., Pesavento, U. & Wang, Z.J., Unsteady aerodynamics of fluttering and tumbling plates, *J. Fluid Mech.*, vol. 541, pp. 65-90, 2005.

[2] Belmonte, A., Eisenberg, H. & Moses, E., From Flutter to Tumble: Inertial Drag and Froude Similarity in Falling Paper, *Physical Review Letters*, vol. 81, no. 2, pp. 345-348, 1998.

[3] Bönisch, S. & Heuveline, V., On the numerical simulation of the unsteady free fall of a solid in a fluid: I. The newtonian case, *Computers & Fluids*, vol. 36, pp. 1434-1445, 2007.

[4] Field,S.B., Klaus,M., Moore, M.G. and F. Nori, M.G., Chaotic dynamics of falling disks, *Nature*, pp. 252-254, 1997.

[5] Fonseca, F. & Herrmann, H.J., Simulation of the sedimentation of a falling oblate ellipsoid, *Physica A*, vol. 345, pp. 341-355, 2005.

[6] Huang, W., Zhou, Q., Wang, F., Lui, H. & Wu, J., Measurements and Visualizations of the Unsteady Flow Filed on a Freely Falling Plate, *Advanced Materials Research*, Vols. 718-720, pp. 1049-1054, 2013.

[7] Hærvig, J., Jensen, A.L., Pedersen, M.C. & Sørensen, H., General observations of the time-dependent flow field around flat plates in free fall, *Proceedings of the ASME-JSME-KSME Joint Fluids Engineering Conference 2015*, Seoul, 2015.

[8] Jensen, A.L. & Hærvig, J., *Extending the Existing Modelling Framework for Non-Spherical Particles to Include Flat Plates in Free Fall - An Experimental and Numerical Investigation of the Unsteady Aerodynamics of Flat Plates*, Aalborg University, Aalborg, 2014.

[9] Maxwell, J.C., On a particular case of the descent of a heavy body in a resisting medium, *Camb. Dublin Math J.*, vol. 9, pp. 115-118, 1853.

[10] Vetchanin, E.V. & Klenov, A.I., Optical measurement of a fluid velocity field around a falling plate, *Vestn. Udmurtsk. Univ. Mat. Mekh. Komp. Nauki*, vol. 25, no. 4, pp. 554-567, 2015.

[11] Willmarth, W.W., Hawk, N.E. & Harvey, R.L., Steady and Unsteady Motions and Wakes of Freely Falling Disks, *The Physics of Fluids*, vol. 7, no. 2, pp. 197-208, 1964.

[12] Zhong, H., Chen, S. & Lee, C., Experimental study of freely falling thin disks: from planar zigzag to spiral, *Physics of Fluids*, vol. 23, pp. 011702-1 - 011702-4, 2011.